The Abdus Salam
International Centre for Theoretical Physics

United Nations
Educational, Scientific and
Cultural Organization

IAEA
International Atomic Energy Agency

2292-3

School and Conference on Analytical and Computational Astrophysics

14 - 25 November - 2011

Magnetohydrodynamics in solar and space physics

Daniel Osvaldo Gomez
Instituto de Astronomia y Fisica del Espacio, Buenos Aires
Argentina

Magnetohydrodynamics in solar and space physics

Daniel Gómez[1,*]

Instituto de Astronomía y Física del Espacio, Casilla de Correo 67, Sucursal 28, (1428) Buenos Aires, Argentina

Luis Martín and Pablo Dmitruk[*]

Departamento de Física, Facultad de Ciencias Exactas y Naturales, Universidad de Buenos Aires, Pabellón I - Ciudad Universitaria, (1428) Buenos Aires, Argentina

Abstract

Because of its proximity, our Sun provides a unique opportunity to perform high resolution observations of its outer layers throughout the whole electromagnetic spectrum. We can also theoretically model most of the fascinating physical phenomena taking place on the Sun, as well as their impact on the solar system.

Many of these phenomena can be properly studied within the framework of magnetohydrodynamics. More specifically, we assume a fully ionized hydrogen plasma and adopt the more comprehensive two-fluid magnetohydrodynamic approximation. For problems such as the solar wind or magnetic loops in the solar corona, which are shaped by a relatively strong mean magnetic field, the reduced magnetohydrodynamic approximation is often used.

We will review the basic features of both two-fluid and one-fluid magnetohydrodynamics, and focus on two particular applications: the turbulent heating of coronal active regions and the dynamics of the solar wind.

Keywords: magnetohydrodynamics, turbulence, solar physics, space physics

[*]Corresponding author, fax: 0054-11-47868114

Email addresses: gomez@iafe.uba.ar (Daniel Gómez), lmartin@df.uba.ar,pdmitruk@df.uba.ar (Luis Martín and Pablo Dmitruk)

[1]Also at the Departamento de Física, Facultad de Ciencias Exactas y Naturales, Universidad de Buenos Aires, Pabellón I - Ciudad Universitaria, (1428) Buenos Aires, Argentina

1. Introduction

Magnetohydrodynamics (MHD) is a reasonable theoretical framework to describe the large-scale dynamics of a plasma, which is also known as one-fluid MHD. Two-fluid effects can be considered through a generalized Ohm's law which includes the Hall current, which is required for phenomena with characteristic length scales comparable or smaller than the ion skin depth c/ω_i (c:speed of light, ω_i: ion plasma frequency). In an ideal plasma, the Hall current causes the magnetic field to become frozen in the electron flow instead of being carried along with the bulk velocity field. Another relevant feature of the ideal Hall MHD description is the self-consistent presence of parallel (to the magnetic field) electric fields, which can therefore accelerate particles.

In astrophysical plasmas, a strong external magnetic field is often present, thus breaking down the isotropy of the problem and eventually causing important changes in the dynamics of these plasmas. For one-fluid MHD, the presence of an external magnetic field gave rise to the so-called reduced MHD approximation (RMHD, see Strauss (1976); Montgomery (1982)). The RMHD equations have been used in a variety of astrophysical applications, such as current sheet formation (van Ballegooijen, 1986; Longcope, & Sudan, 1994), non-stationary reconnection (Hendrix, & van Hoven, 1996; Milano et al., 1999), the dynamics of coronal loops (Gómez, & Ferro Fontán, 1992; Dmitruk, & Gómez, 1999) or the development of turbulence (Dmitruk, Gómez, & Matthaeus, 2003). Dmitruk, Matthaeus, & Oughton (2005) have numerically confirmed the validity of the RMHD equations by directly comparing its predictions with the compressible MHD equations in a turbulent regime. More recently, Gómez, Mahajan & Dmitruk (2008) extended the "reduced" approximation to include two-fluid effects, giving rise to the reduced Hall-MHD description (RHMHD, see also Bian & Tsiklauri (2009)). A comparative study of numerical simulations of the compressible three-dimensional Hall-MHD equations and the reduced approximation, has recently confirmed the validity of the RHMHD description in the asymptotic limit of strong external magnetic fields (Martín, Dmitruk, & Gómez, 2010).

We organize the paper as follows. After introducing the Hall-MHD set of equations in §2, we perform the asymptotic expansion corresponding to the dynamics of a plasma embedded in a strong external magnetic field in §3, and derive the set of RHMHD equations. In §4 we integrate the RHMHD to simulate the development of turbulence in the solar wind. More specifically, we

show that the presence of the Hall effect causes non-negligible changes in the energy power spectrum. We also applied the one-fluid version of these equations (i.e. the RMHD equations) to simulate the internal dynamics of loops of the solar corona. The main results from these simulations are summarized in §5, showing the development of a turbulent regime in these loops, which enhances Joule dissipation to levels consistent with the energy requirements to heat active regions. Finally, in §6 we summarize our conclusions.

2. The Hall-MHD equations

The large-scale dynamics of a multispecies plasma can be described through fluid equations for each species s (see for instance Goldston and Rutherford (1995))

$$\partial_t n_s + \nabla \cdot (n_s \boldsymbol{U}_s) = 0 \quad (1)$$

$$m_s n_s \frac{d\boldsymbol{U}_s}{dt} = n_s q_s (\boldsymbol{E} + \frac{1}{c}\boldsymbol{U}_s \times \boldsymbol{B}) - \nabla p_s + \nabla \cdot \sigma_s + \sum_{s'} R_{ss'} \quad (2)$$

where m_s, q_s are the individual mass and charge of particles of species s, $n_s, \boldsymbol{U}_s, p_s$ are their particle density, velocity field and scalar pressure respectively, while σ_s is the viscous stress tensor and $R_{ss'}$ is the rate of momentum (per unit volume) gained by species s due to collisions with species s'. In the presence of a strong magnetic field, pressure might depart from scalar and become anisotropic (i.e. $p_\parallel \neq p_\perp$), but we are neglecting this effect throughout this paper. The momentum exchange $R_{ss'}$ rate is proportional to the relative speed between both species and is given by

$$R_{ss'} = -m_s n_s \nu_{ss'} (\boldsymbol{U}_s - \boldsymbol{U}_{s'}) \quad (3)$$

where $\nu_{ss'}$ is the collision frequency of an s-particle against particles of species s'. Since the total momentum must of course be conserved, the corresponding exchange rates satisfy $R_{s's} = -R_{ss'}$, from which it follows that collision frequencies must obey $m_s n_s \nu_{ss'} = m_{s'} n_{s'} \nu_{s's}$. The electric current density for a multi-species plasma is defined as

$$\boldsymbol{J} = \sum_s q_s n_s \boldsymbol{U}_s \quad (4)$$

The equations of motion for a fully ionized hydrogen plasma, made of protons of particle mass m and electrons of negligible mass (since $m_e \ll m$)

are given by (Krall & Trivelpiece, 1973)

$$mn\frac{d\boldsymbol{U}}{dt} = en(\boldsymbol{E}+\frac{1}{c}\boldsymbol{U}\times\boldsymbol{B}) - \nabla p_i + \nabla\cdot\sigma + R \tag{5}$$

$$0 = -en(\boldsymbol{E}+\frac{1}{c}\boldsymbol{U}_e\times\boldsymbol{B}) - \nabla p_e - R \tag{6}$$

where $\boldsymbol{U}, \boldsymbol{U}_e$ are the ion and electron flow velocities. The viscous stress tensor for electrons has been neglected, since it is proportional to the particle mass, and the friction force between both species can be written as

$$R = -mn\nu_{ie}(\boldsymbol{U}-\boldsymbol{U}_e) \tag{7}$$

For the fully ionized hydrogen case, the electric current density (see equation (4)) reduces to $\boldsymbol{J} = en(\boldsymbol{U}-\boldsymbol{U}_e)$. Therefore, the friction force R can be expressed as

$$R = -\frac{m\nu_{ie}}{e}\boldsymbol{J} \tag{8}$$

The electron and ion pressures p_e, p_i are assumed to satisfy polytropic laws

$$p_i \propto n^\gamma \tag{9}$$

$$p_e \propto n^\gamma \tag{10}$$

where the particle densities for both species are assumed to be equal because of charge neutrality (i.e. $n_i = n_e = n$). The bulk flow in this two-fluid description is given by the ion flow $\boldsymbol{U}$, which satisfies

$$\partial_t n + \nabla\cdot(n\boldsymbol{U}) = 0 \tag{11}$$

The electric current density relates with the magnetic field through Ampere's law

$$\boldsymbol{J} = \frac{c}{4\pi}\nabla\times\boldsymbol{B} = en(\boldsymbol{U}-\boldsymbol{U}_e) \tag{12}$$

By adding equations (5)-(6) and adopting a Newtonian prescription for the viscous stress tensor (i.e. $\sigma_{ij} = \mu(\partial_i U_j + \partial_j U_i)$, μ: viscosity) we obtain

$$mn\frac{d\boldsymbol{U}}{dt} = \frac{1}{c}\boldsymbol{J}\times\boldsymbol{B} - \nabla p + \mu\nabla^2\boldsymbol{U} \tag{13}$$

where $p = p_i + p_e$. On the other hand, after replacing $\boldsymbol{U}_e = \boldsymbol{U} - \boldsymbol{J}/(en)$ and equation (8) into equation (6), we obtain the so-called "generalized Ohm's law"

$$\boldsymbol{E}+\frac{1}{c}\boldsymbol{U}\times\boldsymbol{B} = \frac{1}{nec}\boldsymbol{J}\times\boldsymbol{B} - \frac{1}{ne}\nabla p_e + \frac{m\nu_{ie}}{e^2 n}\boldsymbol{J} \tag{14}$$

which also expresses the force balance satisfied by the massless electrons. In the last term, we can recognize $e^2 n/(m\nu_{ie})$ as the electric conductivity of a fully ionized hydrogen plasma. The electric and magnetic fields can be cast in terms of the electrostatic potential ϕ and the vector potencial $\boldsymbol{A}$. In particular, the curl of equation (14) yields the induction equation

$$\partial_t \boldsymbol{B} = \nabla \times \left[(\boldsymbol{U} - \frac{1}{en}\boldsymbol{J}) \times \boldsymbol{B} \right] - \nabla \times (\eta \nabla \times \boldsymbol{B}) \tag{15}$$

where

$$\eta = \frac{mc^2 \nu_{ie}}{4\pi e^2 n} \tag{16}$$

is the electric resistivity. Equations (13)-(15) provide the two-fluid description of magnetohydrodynamics. The set of equations is completed by the continuity equation (equation (11)), the adiabatic conditions given by equations (9)-(10) and Ampere's law (equation (12)).

We now turn to a dimensionless version of the preceding set of equations using a typical longitudinal length scale L_0, an ambient density $n = n_0$, a typical value for the magnetic field B_0, a typical velocity equal to the Alfven speed $v_A = B_0/\sqrt{4\pi m n_0}$, and a reference pressure p_0. The equation of motion becomes

$$n\frac{d\boldsymbol{U}}{dt} = (\nabla \times \boldsymbol{B}) \times \boldsymbol{B} - \beta \nabla p + \frac{1}{Re}\nabla^2 \boldsymbol{U} \tag{17}$$

while the induction equation can be written as

$$\partial_t \boldsymbol{B} = \nabla \times \left[(\boldsymbol{U} - \frac{\epsilon}{n}\nabla \times \boldsymbol{B}) \times \boldsymbol{B} \right] + \frac{1}{Rm}\nabla^2 \boldsymbol{B} \tag{18}$$

The various dimensionless coefficients in these equations measure the relative importance of different competing physical effects. The plasma "*beta*"

$$\beta = \frac{p_0}{m_i n_0 v_A^2} \tag{19}$$

is the approximate ratio of gas to magnetic pressure, while the kinetic ($Re = v_A L_0/(\mu/m n_0)$) and magnetic ($Rm = v_A L_0/\eta$) Reynolds numbers express the ratio of convective to dissipative effects in each equation. The Hall parameter

$$\epsilon = \frac{c}{\omega_i L_0} = \sqrt{\frac{m_i c^2}{4\pi e^2 n_0 L_0^2}} \tag{20}$$

expresses the relative importance of the Hall effect. For $\epsilon \to 0$, the induction equation (18) reduces to the one for one-fluid magnetohydrodynamics.

Equations (17)-(18) are also known as the Hall-MHD (HMHD) equations. The HMHD system has been extensively studied in recent years, both analytically and numerically. For instance, Hall-MHD has been applied to advance our understanding of dynamo mechanisms (Mininni, Gómez, & Mahajan, 2003), magnetic reconnection (Mozer, Bale, & Phan, 2002; Smith, 2004; Morales, Dasso, & Gómez, 2005), accretion (Wardle, 1999; Balbus, & Terquem, 2001) or the physics of turbulent regimes (Matthaeus et al., 2003; Mininni, Gómez, & Mahajan, 2005; Galtier, 2006; Dmitruk, & Matthaeus, 2006).

3. Hall-MHD in a strong magnetic field

In the presence of a strong external magnetic field, velocity and magnetic field fluctuations tend to develop fine scale spatial structures across it, while parallel gradients remain comparatively smoother (Shebalin, Matthaeus, & Montgomery, 1983; Oughton, Priest, & Matthaeus, 1994; Matthaeus et al., 1998; Oughton, Matthaeus, & Ghosh, 1998). According to this approximation, the dimensionless magnetic field is of the form (the external field is along $\widehat{\boldsymbol{e}}_{\boldsymbol{z}}$)

$$\boldsymbol{B} = \widehat{\boldsymbol{e}}_{\boldsymbol{z}} + \delta\boldsymbol{B} \quad , \qquad |\delta\boldsymbol{B}| \approx \alpha \ll 1 \tag{21}$$

where α represents the typical tilt of magnetic field lines with respect to the $\widehat{\boldsymbol{e}}_{\boldsymbol{z}}$-direction. Therefore, one expects

$$\nabla_\perp \approx 1 \quad , \qquad \partial_z \approx \alpha \ll 1 \tag{22}$$

To ensure that $\boldsymbol{B}$ remains solenoidal, we assume

$$\boldsymbol{B} = \widehat{\boldsymbol{e}}_{\boldsymbol{z}} + \nabla\times\left(a\widehat{\boldsymbol{e}}_{\boldsymbol{z}} + g\widehat{\boldsymbol{e}}_{\boldsymbol{x}}\right) \tag{23}$$

The velocity field instead, is decomposed into a solenoidal plus an irrotational flow, i.e.

$$\boldsymbol{U} = \nabla\times\left(\varphi\widehat{\boldsymbol{e}}_{\boldsymbol{z}} + f\widehat{\boldsymbol{e}}_{\boldsymbol{x}}\right) + \nabla\psi \tag{24}$$

where the potentials $a(\boldsymbol{r},t)$, $g(\boldsymbol{r},t)$, $\varphi(\boldsymbol{r},t)$ and $f(\boldsymbol{r},t)$ are all assumed of order $\alpha \ll 1$ and $\psi(\boldsymbol{r},t)$ is of order α^2 (see details in Gómez, Mahajan & Dmitruk (2008); and also Bian & Tsiklauri (2009)).

The standard RMHD approximation (Strauss, 1976) only considers the potentials a and φ, which restrict the dynamics to velocity and magnetic field components perpendicular to the external magnetic field. When the Hall effect becomes relevant (i.e. the term proportional to ϵ in equation (18)), potentials f, g and ψ should be added to allow nonzero dynamical field components along $\widehat{\boldsymbol{e}}_{\boldsymbol{z}}$ and therefore capture the helical behavior introduced by this effect.

Assuming also $\partial_t \approx \alpha \ll 1$, we obtain, to first order in α in equations (17)-(18)

$$b + \beta(p_i + p_e) = constant \tag{25}$$

$$\phi + \varphi - \epsilon(b + \beta p_e) = constant \tag{26}$$

which are Bernoulli conditions constraining the pressures and the electrostatic potential.

To order α^2, Eqs. (17)-(18) describe the dynamical evolution of the potentials (i.e. a, φ, g and f)

$$\partial_t a = \partial_z(\varphi - \epsilon b) + [\varphi - \epsilon b, a] + \frac{1}{Rm}\nabla^2 a \tag{27}$$

$$\partial_t \omega = \partial_z j + [\varphi, \omega] - [a, j] + \frac{1}{Re}\nabla^2 \omega \tag{28}$$

$$\partial_t b = \beta_* \partial_z(u - \epsilon j) + [\varphi, b] + \beta_*[u - \epsilon j, a] + \beta_* \frac{1}{Rm}\nabla^2 b \tag{29}$$

$$\partial_t u = \partial_z b + [\varphi, u] - [a, b] + \frac{1}{Re}\nabla^2 u \tag{30}$$

where $j = -\nabla_\perp^2 a$ and $\omega = -\nabla_\perp^2 \varphi$ are, respectively, the parallel current and vorticity components, and $[a, b] = \partial_x a \partial_y b - \partial_y a \partial_x b$ indicate the standard Poisson brackets. The parallel component of the dynamical magnetic field is $b = -\partial_y g$, and that of the velocity field is $u = -\partial_y f$. The coefficient β_* is

$$\beta_* = \frac{\gamma\beta}{1 + \gamma\beta} \tag{31}$$

where β is the coefficient defined in equation (19) and γ is the polytropic index (see equations (9)-(10)). In summary, the set of equations (27)-(30) describe the dynamical evolution of a Hall plasma embedded in a strong external magnetic field.

Just as for three-dimensional Hall-MHD, this set of equations display three ideal invariants: the energy

$$E = \frac{1}{2}\int d^3r\ (|\boldsymbol{U}|^2 + |\boldsymbol{B}|^2) = \frac{1}{2}\int d^3r\ (|\nabla_\perp \varphi|^2 + |\nabla_\perp a|^2 + u^2 + b^2)\ , \quad (32)$$

the magnetic helicity

$$H_m = \frac{1}{2}\int d^3r\ (\boldsymbol{A}\cdot\boldsymbol{B}) = \int d^3r\ ab\ , \quad (33)$$

and the hybrid helicity (Turner, 1983; Mahajan, & Yoshida, 2000)

$$H_h = \frac{1}{2}\int d^3r\ (\boldsymbol{A}+\epsilon\boldsymbol{U})\cdot(\boldsymbol{B}+\epsilon\boldsymbol{\Omega}) = \int d^3r\ [ab + \epsilon(a\omega + ub) + \epsilon^2 u\omega)] \quad (34)$$

where $\boldsymbol{\Omega} = \nabla\times\boldsymbol{U}$ is the vorticity vector field.

4. Application of RHMHD to solar wind turbulence

The relative importance of the Hall effect in the Hall-MHD equations (i.e. equations (17)-(18)) is determined by the coefficient ϵ, which is only present in equation (18). From the expresion of ϵ in equation (20), we find that the Hall effect must become non-negligible in sufficiently low density plasmas. One of the many low-density astrophysical plasmas for which the Hall effect is known to be relevant is the solar wind, and it becomes progressively more important as we move away from the Sun. Also, the solar wind plasma is permeated by an external magnetic field (although the magnetic fluctuations can be a non-negligible fraction of the external field).

To study the role of the Hall effect on the energy power spectrum, we integrate equations (27)-(30) numerically. We assume periodicity for the lateral boundary conditions, and specify the velocity fields at the boundaries $z = 0$ and $z = L$ (for a detailed description, see Dmitruk, Gómez, & Matthaeus (2003)). These boundary motions pump energy into the system and drives it into a turbulent regime. We use a pseudo-spectral technique with dealiasing for the perpendicular spatial derivatives and finite differences for the (much smoother) $\widehat{\boldsymbol{e}}_{\boldsymbol{z}}$-derivatives. We start all our simulations with trivial initial conditions (i.e. $a = \varphi = u = b = 0$).

To study the role of the Hall current in a plasma permeated by a strong magnetic field, we performed a set of simulations with different values of the

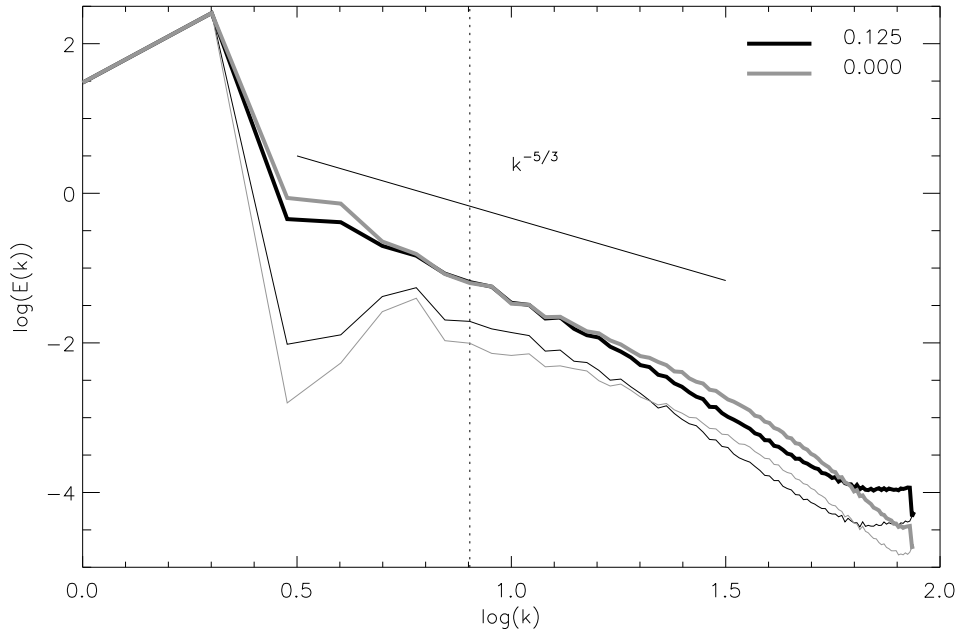

Figure 1: Energy power spectra for $\epsilon = 0.000$ (gray) and $\epsilon = 0.125$ (black). The Kolmogorov slope is displayed for reference, and the vertical dashed line indicates the location of $k_\epsilon = 1/\epsilon$ for $\epsilon = 0.125$. The dotted lines show the power spectra for the corresponding kinetic energies.

Hall parameter (see details in Gómez, Mahajan & Dmitruk (2008)). Among the results arising from these simulations, we find that the fraction of kinetic to total energy increases monotonically with the Hall coefficient ϵ.

In the MHD limit ($\epsilon = 0$), the total energy reduces to (Eq. (32))

$$E_{perp} = \frac{1}{2} \int d^3r \ (|\nabla_\perp \varphi|^2 + |\nabla_\perp a|^2) \tag{35}$$

while for the general case ($\epsilon \neq 0$) there is a fraction of the total energy directly associated to the parallel degrees of freedom

$$E_{par} = \frac{1}{2} \int d^3r \ (u^2 + b^2) \tag{36}$$

The fraction E_{par}/E_{tot} is also observed to increase monotonically with ϵ, even though we are not pumping parallel energy from the boundaries. Parallel fluctuations are generated by the perpendicular part of the dynamics (i.e. by a and φ) via terms proportional to ϵ in equation (29).

We expect the Hall current to affect the dynamics of spatial patterns whose sizes are of the order of the ion skin depth (i.e. c/w_i) or smaller. According to Equation (20), this typical size corresponds to a $k_\epsilon = 1/\epsilon$. In Figure 1 we compare the spectral distributions of energy for $\epsilon = 0.000$ and $\epsilon = 0.125$, once a stationary turbulent regime is reached for each of these simulations. Even though these numerical simulations have only a moderate spatial resolution of $256 \times 256 \times 30$, the energy spectra are consistent with the slope predicted by Kolmogorov (i.e. $E_k \propto k^{-5/3}$) at intermediate and large scales (i.e. intermediate and small values of k). For the simulation corresponding to $\epsilon = 0.125$, we also find that the kinetic energy spectrum becomes a fair fraction of the total energy spectrum for $k \geq k_\epsilon$.

We need simulations at much higher spatial resolution to make quantitative asessments about the energy power spectra, but the behavior at small scales (i.e. $k < k_\epsilon$) is clearly affected by the presence of the Hall term. The RHMHD framework has been numerically tested against the more general compressible Hall-MHD description (Martín, Dmitruk, & Gómez, 2010). The results show that the degree of agreement between both sets of simulations is very high when the various assumptions for RHMHD are satisfied, thus rendering RHMHD as a valid approximation of Hall-MHD in the presence of strong external magnetic fields.

5. Application of RMHD to coronal heating

Another application of the reduced approximation to an astrophysical problem, is the simulation of magnetic loops of the solar corona, to study the heating of the plasma confined in coronal magnetic structures. To model the internal dynamics of coronal loops in solar (or stellar) active regions, we assume these loops to be relatively homogeneous bundles of fieldlines, with their footpoints deeply rooted into the photosphere. Individual fieldlines are moved around by subphotospheric convective motions, which in turn generate magnetic stresses in the coronal portion of the loop. We therefore consider a magnetic loop with length L and cross section $2\pi l_p \times 2\pi l_p$, where l_p is the lengthscale of typical subphotospheric motions. For elongated loops, *i.e.* such that $2\pi l_p << L$, we neglect toroidal effects. The main magnetic field $\mathbf{B_0}$ is assumed to be uniform and parallel to the axis of the loop (the z axis) and the perpendicular planes at $z = 0$ and $z = L$ correspond to the photospheric footpoints. For the coronal plasma, the Hall effect is actually negligible, so we simply integrate the RMHD equations (i.e. $\epsilon = 0.000$).

As boundary conditions, we assume $\psi(z = 0) = 0$ and $\psi(z = L) = \Psi(x, y)$ where the stream function $\Psi(x, y)$ describes stationary and incompressible footpoint motions on the photospheric plane. We specify the Fourier components of $\Psi(x, y)$ as $\Psi_{\mathbf{k}} = \Psi_0$ inside the ring $3 < l_p|k| < 4$ on the Fourier plane, and $\Psi_{\mathbf{k}} = 0$ elsewhere, to simulate a stationary and isotropic pattern of photospheric granular motions of diameters between $2\pi l_p/4$ and $2\pi l_p/3$. The strength Ψ_0 is proportional to a typical photospheric velocity $V_p \approx 1\ km.s^{-1}$. The typical timescale associated to these driving motions, is the eddy turnover time, which is defined as $t_p = l_p/V_p \approx 10^3\ sec$. We choose a narrowband and non-random forcing to make sure that the broadband energy spectra and the signatures of intermittency that we obtain are exclusively determined by the nonlinear nature of the MHD equations.

In Figure 2 we show the results obtained from a simulation extending from $t = 0$ to $t = 100t_A$, where $t_A = L/v_A$ is the Alfven time of the loop. The upper panel shows the kinetic (E_U, thin trace) and total energy ($E = E_U + E_B$, thick trace). We can see that after about ten Alfven times, the energy reaches a stationary regime, since the work done by footpoint motions statistically (i.e. in time average) reaches an equilibrium with the dissipative processes (electric resistivity and fluid viscosity). In this stationary regime most of the energy is magnetic, while kinetic energy is only about 5% of the total. In the lower panel, we show the dissipation rate (D, thick trace) and the

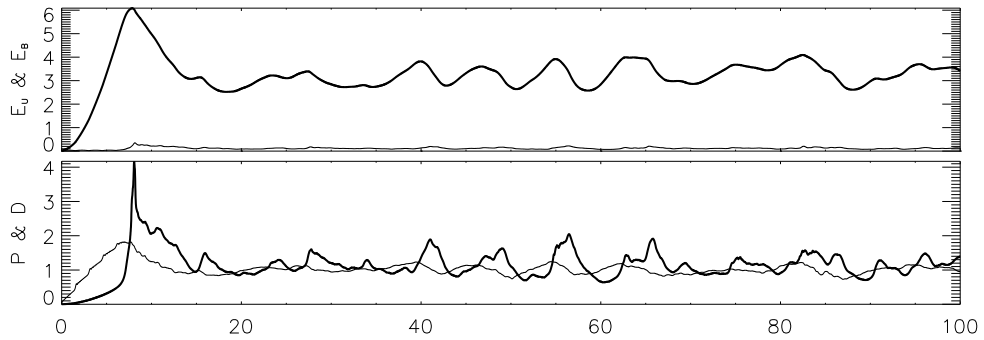

Figure 2: Energy and dissipation rate time series. **Upper panel**: Kinetic energy (thin), and total energy (thick). **Lower panel**: Energy dissipation rate (thick) and Poynting flux (thin).

incoming Poynting flux (P, thin trace), showing that their time averages are approximately equal.

The observed stationary equilibrium has been shown to correspond to a turbulent regime (Gómez, & Ferro Fontán, 1988, 1992), and therefore the associated energy cascade bridges the gap between the large spatial scales where energy is injected by footpoint motions, to the much smaller scales where it dissipates (see Dmitruk, & Gómez (1997)). The dependence of the stationary dissipation rate $\epsilon =< D >=< P >$ ($< \ldots >$: time average) with the physical parameters of the loop is (Dmitruk, & Gómez (1999))

$$\epsilon \propto \frac{\rho l_p^2}{t_A^3}(\frac{t_A}{t_p})^{\frac{3}{2}} \tag{37}$$

In Figure 2 we can clearly observe the spiky nature of these time series, which is the result of the intermittency arising in turbulent regimes. Dmitruk, Gómez, & DeLuca (1998) associated these spikes of energy dissipation with Parker's *nanoflares* (see Parker (1988)) and studied the statistical distribution of these dissipation events. The main result from this statistical study (see also Gómez, & Dmitruk (2008)) is that the number of nanoflares as a function of their energies $N(E)$ follows a power law $N(E) \approx E^{-3/2}$, which is remarkably comparable to the result obtained for larger dissipation events (such as microflares and flares), gathering a large number of observational studies and reported by Aschwanden (2004).

6. Conclusions

In this presentation we reviewed the basic features of two-fluid magnetohydrodynamics as a valid theoretical framework for astrophysical and space plasmas. Even though two-fluid MHD is aimed at theoretically describing the relatively large-scale behavior of plasmas, it does nonetheless retain the effects of the Hall current at scales comparable or smaller than the ion skin-depth. For plasmas permeated by relatively strong external magnetic fields, we introduce the reader to the so-called reduced magnetohydrodynamic approximation, which takes advantage of the much smoother spatial structure of these plasmas along magnetic fieldlines.

We also present numerical results of the reduced MHD equations which are relevant to the following two astrophysical problems: the turbulent dynamics of the solar wind plasma and the turbulent heating of coronal active regions. In the solar wind plasma, the Hall effect becomes progressively more important as we move away from the Sun. Our RHMHD simulations show that the Hall effect is able to produce measurable changes in the energy power spectrum. In particular, the ratio of kinetic to total energy increases with the Hall coefficient ϵ, as well as the ratio of parallel to total energy (Gómez, Mahajan & Dmitruk, 2008).

We have also shown numerical results from RMHD simulations (the Hall effect is not likely to be relevant in the coronal plasma) of the internal dynamics of magnetic loops of the solar corona. These simulations show the development of a magnetically dominated and stationary turbulent regime inside the loop, as a result of the persistent action of convective subphotospheric motions. The mean value of the heating rate arising from these simulations is of the same order of magnitude of the main cooling rates in coronal active regions (Dmitruk, & Gómez, 1997), namely, radiative losses and thermal conductivity to the chromosphere. Superimposed to this stationary heating rate, simulations also show the ubiquitous presence of spiky heating events, as a result of the intermittent nature of turbulence. The statistics of these heating events or *nanoflares* (see Dmitruk, Gómez, & DeLuca (1998)), is remarkably similar to the one obtained for the much larger dissipation events, known as *flares* (see Aschwanden (2004)).

7. References

Aschwanden, M.J., in *Physics of the Solar Corona. An Introduction*, Springer-Verlag (Berlin), 2004.

Balbus, S.A., & Terquem, C., *Astrophys. J.*, 552, 235, 2001.

Bian, N.H., & Tsiklauri, D., *Phys. Plasmas*, 16, 064503, 2009.

Dmitruk, P., & Matthaeus, W.H., *Phys. Plasmas*, 13, 2307, 2006.

Dmitruk, P., Matthaeus, W.H., & Oughton, S., *Phys. Plasmas*, 12, 112304, 2005.

Dmitruk, P., Gómez, D.O., & Matthaeus, W.H., *Phys. Plasmas*, 10, 3584, 2003.

Dmitruk, P., & Gómez, D.O., *Astrophys. J.*, 527, L63, 1999.

Dmitruk, P., Gómez, D.O., & DeLuca, E., *Astrophys. J.*, 505, 974, 1998.

Dmitruk, P., & Gómez, D.O., *Astrophys. J.*, 484, L83, 1997.

Galtier, S., *J. Plasma Phys.*, 72, 721, 2006.

Goldston, R.J., & Rutherford, P.H., *Introduction to Plasma Physics*, IOP Publ. (Bristol & Philadelphia), 1995.

Gómez, D.O., Mahajan, S.M., & Dmitruk, P., *Phys. Plasmas*, 15, 102303, 2008.

Gómez, D.O., & Dmitruk, P., in "Proc. IAU Symp. 247: Waves and Oscillations in the Solar Atmosphere", (Eds. R. Erdelyi & C.A. Mendoza-Briceño), 269, 2008.

Gómez, D.O., & Ferro Fontán, C., *Astrophys. J.*, 394, 662, 1992.

Gómez, D.O., & Ferro Fontán, C., *Solar Phys.*, 116, 33, 1988.

Hendrix, D.L., & van Hoven, G., *Astrophys. J.*, 467, 887, 1996.

Krall, N.A., & Trivelpiece, A.W. in *Principles of Plasma Physics* (McGraw-Hill, New York, 1973), p. 89.

Longcope, D.W., & Sudan, R.N., *Astrophys. J.*, 437, 491, 1994.

Mahajan, S.M., & Yoshida, Z., *Phys. Plasmas*, 7, 635, 2000.

Martín, L.N., Dmitruk, P., & Gómez, D.O., *Phys. Plasmas*, 17, 112304, 2010.

Matthaeus, W.H., Dmitruk, P., Smith, D., Ghosh, S., & Oughton, S., *Geophys. Res. Lett.*, 30, 2104, 2003.

Matthaeus, W.H., Oughton, S., Ghosh, S., & Hossain, M., *Phys. Rev. Lett.*, 81, 256, 1998.

Milano, L., Dmitruk, P., Mandrini, C.H., Gómez, D.O., & Demoulin, P., *Astrophys. J.*, 521, 889, 1999.

Mininni, P.D., Gómez, D.O., & Mahajan, S.M., *Astrophys. J.*, 619, 1019, 2005.

Mininni, P.D., Gómez, D.O., & Mahajan, S.M., *Astrophys. J.*, 584, 1120, 2003.

Morales, L.F., Dasso, S., & Gómez, D.O., *J. Geophys. Res.*, 110, A04204, 2005.

Montgomery, D.C., *Phys. Scr.*, T2/1, 83, 1982.

Mozer, F., Bale, S., & Phan, T.D., *Phys. Rev. Lett.*, 89, 015002, 2002.

Oughton, S., Matthaeus, W.H., & Ghosh, S., *Phys. Plasmas*, 5, 4235, 1998.

Oughton, S., Priest, E.R., & Matthaeus, W.H., *J. Fluid Mech.*, 280, 95, 1994.

Parker, E.N., *Astrophys. J.*, 330, 474, 1988.

Shebalin, J.V., Matthaeus, W.H., & Montgomery, D., *J. Plasma Phys.*, 29, 525, 1983.

Smith, D., Ghosh, S., Dmitruk, P., & Matthaeus, W.H., *Geophys. Res. Lett.*, 31, 02805, 2004.

Strauss, H., *Phys. Fluids*, 19, 134, 1976.

Turner, L., *IEEE Trans. Plasma Sci.*, PS14, 849, 1983.

van Ballegooijen, A.A., *Astrophys. J.*, 311, 1001, 1986.

Wardle, M., *Mon. Not. R.A.S.*, 303, 239, 1999.